

# Analytical Methods

Accepted Manuscript



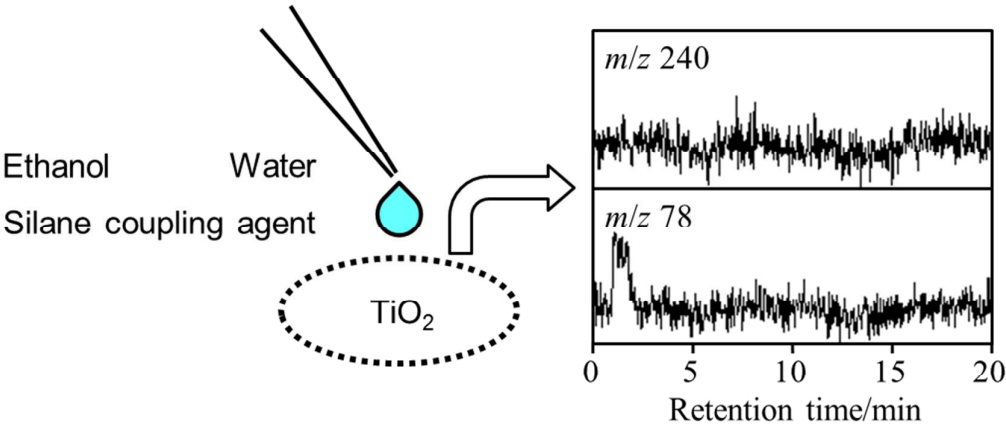
This is an *Accepted Manuscript*, which has been through the Royal Society of Chemistry peer review process and has been accepted for publication.

*Accepted Manuscripts* are published online shortly after acceptance, before technical editing, formatting and proof reading. Using this free service, authors can make their results available to the community, in citable form, before we publish the edited article. We will replace this *Accepted Manuscript* with the edited and formatted *Advance Article* as soon as it is available.

You can find more information about *Accepted Manuscripts* in the [Information for Authors](#).

Please note that technical editing may introduce minor changes to the text and/or graphics, which may alter content. The journal's standard [Terms & Conditions](#) and the [Ethical guidelines](#) still apply. In no event shall the Royal Society of Chemistry be held responsible for any errors or omissions in this *Accepted Manuscript* or any consequences arising from the use of any information it contains.

<For Table of Contents>



LI/TOFMS was applied to the measurement of pyrolysis products generated from silanized  $\text{TiO}_2$  nanoparticles.

**Application of laser ionization mass spectrometry  
for the analysis of pyrolysis products from TiO<sub>2</sub>  
nanoparticles treated with a silane coupling agent**

**Takaaki Fujii and Tomohiro Uchimura<sup>\*</sup>**

Department of Materials Science and Engineering, Graduate School of Engineering, University  
of Fukui, 3-9-1 Bunkyo, Fukui 910-8507, Japan

<sup>\*</sup> To whom correspondence should be addressed. E-mail: [uchimura@matse.u-fukui.ac.jp](mailto:uchimura@matse.u-fukui.ac.jp)

**Abstract**

Laser ionization time-of-flight mass spectrometry (LI/TOFMS) was applied to the analysis of pyrolysis products from TiO<sub>2</sub> nanoparticles treated with phenyltriethoxysilane (PTES). The first step was to measure the decomposition products from silanized TiO<sub>2</sub> nanoparticles by gradual heating in a gas chromatograph (GC) oven. As a result, a molecular ion peak was not observed for PTES, while a peak for the benzene ion was prominent. However, a molecular ion peak and some fragment ion peaks did appear in the mass spectrum of PTES, whereas a peak for the benzene ion did not. These results indicated the existence of compounds that were different from PTES on the surface of the silanized TiO<sub>2</sub> nanoparticles that were used in the present study. In addition, a toluene ion peak was observed when heating with a GC oven, but that of phenol, rather than toluene, was confirmed when a pyrolyzer was used for rapid heating. A plausible explanation for these results could be the existence of water in the vicinity of silanized TiO<sub>2</sub> nanoparticles when the pyrolysis products were generated. In the present study, the products generated by heating a glass filter paper or TiO<sub>2</sub> nanoparticles where PTES had been dropped were also measured using a pyrolyzer in order to confirm whether the adsorption conditions could be identified. As a result, a peak for benzene, but not for PTES, was observed by heating TiO<sub>2</sub> nanoparticles, while a molecular ion of PTES was prominent when a glass filter paper was heated. These results suggest that the present method can reveal the differences in silane coupling agents, and can be used to evaluate whether these agents remain on the target sample or have been chemisorbed.

## Introduction

Titanium dioxide ( $\text{TiO}_2$ ) nanoparticles, which are known as a white pigment, have several outstanding properties such as a brilliant whiteness, a high degree of hiding power, and a high refractive index. Therefore, these have been applied to a wide array of materials such as paints, inks, cosmetics, and sunscreens.<sup>1,2</sup> In addition, their photocatalytic effect is used to purify environmental pollutants.<sup>3</sup> Several analytical methods are commonly used for the analysis of metal oxide nanoparticles: microscopy (scanning electron microscopy, SEM, and transmission electron microscopy, TEM),<sup>4-6</sup> spectroscopy (Fourier transform infrared, FTIR,<sup>4</sup> and nuclear magnetic resonance, NMR),<sup>7,8</sup> and, crystallography (X-ray diffraction, XRD).<sup>5,9</sup> Several reports have documented the evaluation of  $\text{TiO}_2$  nanoparticles via the development of analytical methods for the thermal decomposition of organic compounds using gas chromatography (GC),<sup>10</sup> and others have provided analysis of the products from the surface reaction of  $\text{TiO}_2$  as measured by FTIR or mass spectrometry (MS).<sup>11</sup>

In order to prevent the aggregation of metal oxide nanoparticles such as  $\text{TiO}_2$ , surfaces are usually coated with organic compounds.<sup>6,12,13</sup> This coating improves the dispersibility of particles and narrows the size distribution. Thus, it is important to evaluate the adsorption conditions of the organic compounds that are used to coat the surfaces of metal oxide nanoparticles. Though diffuse reflectance infrared Fourier transform spectroscopy (DRIFTS) has been used for the analysis of adsorbed compounds on the metal oxide nanoparticles,<sup>14,15</sup> it is sometimes difficult to dictate the adsorption conditions of organic compounds. Therefore, metal oxide nanoparticles with a high dispersibility are often prepared based on a rule of thumb. With respect to MS, only the measurement of pyrene used to cover  $\text{TiO}_2$  has been reported.<sup>16</sup> The

development of analytical techniques that could reveal the conditions that govern the adsorption of organic compounds on metal oxide nanoparticles would be helpful in understanding the relationships between the properties of modified metal oxide nanoparticles, which could lead to improvements in commercial TiO<sub>2</sub> products.

In the present study, laser ionization time-of-flight mass spectrometry (LI/TOFMS) was applied to the measurement of pyrolysis products generated from silanized TiO<sub>2</sub> nanoparticles. This technique uses an ultraviolet (UV) laser for ionization and offers highly selective analysis for aromatic hydrocarbons.<sup>17-25</sup> The first step was to measure the mass spectrum of phenyltriethoxysilane (PTES), which is one of the silane coupling agents. Next, the pyrolysis products from silanized TiO<sub>2</sub> nanoparticles were investigated. Several groups have reported vaporized compounds from various samples directly measured by MS,<sup>26,27</sup> or measured by thermal desorption and/or pyrolysis GC-MS.<sup>28-35</sup> In the present study, we applied two types of heating systems: a GC oven was used for gradual heating and a Curie-point pyrolyzer was used for rapid heating. Moreover, the possibility of the identification of desorbed PTES with the substrates was verified.

## Experimental

### Materials

TiO<sub>2</sub> nanoparticles (mean particle diameter ca. 250 nm, rutile), including some that had been silanized, were kindly provided by Y. Tanaka and T. Hizawa (Central Research Laboratories, DIC, Japan). Briefly, PTES (Tokyo Chemical Industry) was used as a silane coupling agent.

After silanization, the TiO<sub>2</sub> nanoparticles were washed with deionized water to remove the unreacted PTES, and were dried in an oven at 90 °C. The weights of the PTES used for the treatment of TiO<sub>2</sub> nanoparticles were either 1.5 mg/g-TiO<sub>2</sub> or 6.1 mg/g-TiO<sub>2</sub>. The ratio of the surface coverage was estimated by the manufacturer to be 50 and 200%, respectively, and was calculated from the ratio of the active surface area of TiO<sub>2</sub> nanoparticles, which was assumed to be 1/10 of the entire surface area—the smallest coating area of PTES—all of which was assumed to be consumed for coating. At a glance, the PTES with a weight of 6.1 mg/g-TiO<sub>2</sub> seemed to have dispersed better than the 1.5 mg/g-TiO<sub>2</sub> version.

### Sample introduction

Two different methods were applied to the heating of the sample in the present study. In the first, the TiO<sub>2</sub> nanoparticles were set in a GC oven (Agilent Technologies 7890A), and were gradually heated to introduce the vaporized components into TOFMS. Figure 1 is a schematic representation of the first method used in the present study. A sample-holding part was constructed by the combination of a union tee, a reducing union, and a cap, all of which were made of stainless steel (Swagelok). A 4 mg powdery sample was set in a cap and then a glass fiber filter (GF-75, Advantec, Japan) was cut based on the diameter of the cap, which was then used as a cover in order to prevent the sample from scattering. An inert metal column (Ultra ALLOY, 0.25 mm i.d., Frontier Laboratory, Japan) was connected to the sample-holding part (9 m in length before the sample-holding part and 1 m in length after the part). The GC oven temperature for pyrolysis was programmed from 40 °C to 70 °C at 60 °C/min, to 170 °C at

40 °C/min, to 290 °C at 30 °C/min, and to 450 °C at 20 °C/min and held for 10 min. Nitrogen was used as a carrier gas at 1 mL/min.

The second sample heating technique used a portable Curie-point injector (JCI-22, Japan Analytical Industry). The analytical instrument using the injector was previously reported,<sup>35</sup> and is only briefly described here. Approximately 1 mg of silanized TiO<sub>2</sub> nanoparticles was used in the present study, and non-silanized nanoparticles were used to confirm a blank background. The temperatures for pyrolysis were 333, 445, and 500 °C for non-silanized and 6.1 mg/g-TiO<sub>2</sub> nanoparticles, and 333, 386, 445, and 500 °C for 1.5 mg/g-TiO<sub>2</sub> nanoparticles. The holding time for pyrolysis was 5 sec. The temperature of an injection port of the GC was either 300 or 320 °C. A 30 m × 0.32 mm × 0.25 µm HP-5 (Agilent Technologies) was used for the GC separation. The GC oven temperature for separation was programmed from 40 °C and held for 3 min, and to 320 °C at 20 °C/min and held for 3 min. Nitrogen was used as a carrier gas for the GC separation at 1 mL/min.

An evaluation of the desorption of PTES was also demonstrated in the present study. First, a 0.5% PTES (Shin-Etsu Silicone, Japan) solution in ethanol was prepared, and then it was mixed with deionized water (1/9, v/v). A 1.4 µL sample of the solution was dropped onto 1 mg TiO<sub>2</sub> nanoparticles on a pyrofoil; the volume was determined to a PTES equivalent of 6.1 mg/g-TiO<sub>2</sub> nanoparticles. Also, the same amount of solution was also dropped onto a 3 × 8 mm glass filter paper (GF-75, Advantec) to create a model for physisorption. In both cases, the pyrofoil was quickly folded after dropping and was set to a pyrolyzer.

## LI/TOFMS



The analyte generated by the above-mentioned methods was introduced into a linear-type TOFMS, which is now commercially available (Hikari-GK, HGK-1, drift length 60 cm, Fukuoka, Japan). A deactivated capillary column (i.d., 0.32 mm; GL Sciences) was connected to a TOFMS: 0.3 m in length when using a GC oven for heating or 1 m in length when using a pyrolyzer. The capillary column was connected to an inert metal column in the former case, and connected to an HP-5 column in the latter case. The temperature of the transfer line between the GC and the TOFMS was kept at 300 °C. The fourth harmonic emission of a Nd:YAG laser (Rayture Systems, GAIA II, 30 Hz, 20-50  $\mu$ J, 4 ns, Tokyo, Japan) was used as the ionization laser. The laser beam was focused with a plano-convex lens ( $f = 200$  mm). A microchannel plate detector (Hamamatsu Photonics, F4655-11, Shizuoka, Japan) was used as an ion detector. Either a digital oscilloscope (Tektronix, TDS5104, 1 GHz) or a digitizer (Acqiris/Agilent Technologies, AP240, 1 GHz) was used as a signal recorder. The obtained data were processed by a program constructed in-house using LabVIEW (National Instruments).

## Results and discussion

### Mass spectrum of PTES

The mass spectrum of PTES was first measured, and the results are shown in Figure 2. In this experiment, the sample was introduced into the TOFMS as follows. The PTES was placed in a container at room temperature, and vaporized molecules were introduced into the TOFMS through a deactivated capillary column, with the temperature maintained at 300 °C, which was the same as the above-mentioned transfer line. In the mass spectrum, a molecular ion peak ( $m/z$  240) could be clearly noted. Several fragment peaks were also confirmed, but a peak for

benzene ( $m/z$  78) was not detected, which was observed as a pyrolysis product from the  $\text{TiO}_2$  nanoparticles treated with PTES, and will be discussed later. Incidentally, peaks with higher masses, such as the condensation products (oligomer) of PTES, were not observed under these experimental conditions.

### Heating with a GC oven

The peaks of PTES could be observed via LI/TOFMS, which then was applied to the detection of pyrolysis products from silanized  $\text{TiO}_2$  nanoparticles. At first, the sample was heated using a GC oven. Figure 3 shows the two-dimensional displays of the pyrolysis products obtained from the samples of 1.5 mg/g- $\text{TiO}_2$  and 6.1 mg/g- $\text{TiO}_2$  nanoparticles.

Among the obtained peaks, a peak at  $m/z$  78 was prominent. The peak was derived from benzene, due to the observed mass and the selectivity of the laser ionization. This was because the 266-nm nanosecond laser used in the present study can selectively ionize aromatic compounds, but not aliphatic ones. Benzene, however, has a low degree of ionization efficiency.<sup>36,37</sup> Therefore, a large amount of benzene was generated by heating the silanized  $\text{TiO}_2$  nanoparticles. In addition, as shown in Fig. 2, benzene cannot be detected from PTES, even when it is heated. These results suggest that the PTES did not remain on the surface of  $\text{TiO}_2$  nanoparticles since it was reacted with  $\text{TiO}_2$  nanoparticles and/or was washed, and benzene was generated from the surface of the nanoparticles as a pyrolysis product. The adsorption condition of PTES and the observed peaks will be discussed later.

When heating with a GC oven, a few characteristic shapes were found at specific time courses. For example, as shown in Fig. 3, the time course for benzene showed a bimodal shape from 1.5 mg/g-TiO<sub>2</sub> nanoparticles, while the earlier peak seemed to be enhanced when heating 6.1 mg/g-TiO<sub>2</sub> nanoparticles. The origin of each peak remains unknown, but one theory holds that a later peak indicates the generation of benzene from the surface of the TiO<sub>2</sub> nanoparticles while an earlier peak indicates benzene being generated from the condensation products of a silane coupling agent. These agents were located at a slightly distant place from the surface and were generated when the modified TiO<sub>2</sub> nanoparticles were prepared. However, the time courses obtained at *m/z* 118 and 132 by both TiO<sub>2</sub> nanoparticles exhibited unimodal shapes, although the peak time differed: 14 min (oven temperature 430 °C) at *m/z* 118 and 12.5 min (oven temperature 400 °C) at *m/z* 132. The relationship between the ratio of coverage and the shape of the time course should be discussed in future studies. A better understanding of that relationship could help elucidate the binding conditions between TiO<sub>2</sub> nanoparticles and PTES.

### Heating with a pyrolyzer

As shown in Figure 3, when the silanized TiO<sub>2</sub> nanoparticles were gradually heated in a GC oven, the induced pyrolysis products were observed for an extended period of time. In order to confirm the pyrolysis components, GC/LI/TOFMS combined with a Curie-point pyrolyzer was applied. First, the optimal temperature for the measurement was determined by investigating two-dimensional displays by changing the pyrolysis temperature. As a result, a temperature of 445 °C resulted in the greatest number of peaks and the signal intensities were stronger for both 1.5 mg/g-TiO<sub>2</sub> and 6.1 mg/g-TiO<sub>2</sub> nanoparticles. Lower temperatures seemed insufficient for the

pyrolysis of coated compounds, while pyrolysis proceeded with compounds that contained no phenyl groups at higher temperatures. Therefore, these compounds could not be ionized by the UV laser used in the present study.

Figure 4 shows a two-dimensional display of the pyrolysis products from 6.1 mg/g-TiO<sub>2</sub> nanoparticles obtained by Py-GC/LI/TOFMS at a temperature of 445 °C. Several peaks were either assigned according to a comparison of results obtained by measuring a standard mixture of polycyclic aromatic hydrocarbons, or they were assigned according to the candidate chemical formulae that also are indicated in the figure. Similar to the studies using a GC oven, a molecular ion peak of PTES could not be detected, but a peak from benzene was clearly observed. It is noteworthy that a peak at  $m/z$  94, rather than  $m/z$  92, was observed using a pyrolyzer, as shown in Figure 4, which was in opposition to the results when using a GC oven, as shown in Figure 3. Based on the optical selectivity of laser ionization for aromatic hydrocarbons, the candidates of  $m/z$  92 and 94 were toluene and phenol, respectively. One possible reason for the difference in the pyrolysis products was the existence of water molecules in the reaction atmosphere when each product was generated. A further explanation is that when the silanized TiO<sub>2</sub> nanoparticles were gradually heated in a GC oven, the detection temperature for toluene exceeded 200 °C, and therefore water molecules no longer existed around the TiO<sub>2</sub> nanoparticles. When a pyrolyzer was used, however, water molecules existed even when the pyrolysis temperature reached 445 °C, which resulted in the generation of phenol. Therefore, the existence of water molecules might have an influence on the pyrolysis products, which should be acknowledged in the evaluation of coated metal oxide nanoparticles.

## Identification of adsorption conditions

As shown in Figure 2, the molecular ion peak of PTES can be observed by LI/TOFMS. However, the corresponding peak was not observed for the silanized TiO<sub>2</sub> nanoparticles, as shown in Figures 3 and 4. Therefore, it was assumed that unreacted PTES did not remain on the surface of TiO<sub>2</sub> nanoparticles. If PTES remains on the surface, the molecular ion peak should be measured following heating, which can surely be differentiated from the pyrolysis products generated from chemisorbed substances. That is to say, the present technique can identify whether a silane coupling agent exists as a chemisorbed form or a physisorbed form. In order to confirm this, PTES diluted with ethanol and water was dropped onto TiO<sub>2</sub> nanoparticles or onto a glass filter paper, and then the vaporized components were measured. A glass filter paper was employed in the assumption that the number of active sites that can be reacted with PTES should be much smaller than that of TiO<sub>2</sub> nanoparticles, and therefore unreacted PTES would be detectable. Figure 5 shows the mass chromatograms of pyrolysis products constructed at  $m/z$  78 and 240 obtained from either PTES dropped onto TiO<sub>2</sub> nanoparticles or onto a glass filter paper. From the TiO<sub>2</sub> nanoparticles, the molecular ion peak of PTES was not detected and the peak from benzene was prominent. The obtained results agreed with those shown in Figures 3 and 4. The PTES reacted rapidly with the TiO<sub>2</sub> nanoparticles to form a chemisorbed species. However, from the PTES dropped onto glass filter paper, the peak of PTES was clearly detected and that of benzene was only slightly observed. These results indicate that a portion of the PTES reacted to form a chemisorbed species on the glass filter paper and a portion remained as a physisorbed entity. In this manner, this method can detect the unreacted PTES, which makes it useful in evaluating the adsorption conditions of silane coupling agents at each step of the coating of metal oxide nanoparticles.

1  
2  
3  
4  
5  
6  
7  
8  
9  
10  
11  
12  
13  
14  
15  
16  
17  
18  
19  
20  
21  
22  
23  
24  
25  
26  
27  
28  
29  
30  
31  
32  
33  
34  
35  
36  
37  
38  
39  
40  
41  
42  
43  
44  
45  
46  
47  
48  
49  
50  
51  
52  
53  
54  
55  
56  
57  
58  
59  
60

**Conclusions**

In the present study, the pyrolysis products from TiO<sub>2</sub> nanoparticles treated with PTES were measured using LI/TOFMS. The detection of benzene as a pyrolysis product was strong. Moreover, the pyrolysis products were different based on the heating speed, mainly due to the existence of water molecules. Distinctions were demonstrated between the chemisorption and physisorption of PTES with a substrate surface. Therefore, LI/TOFMS can reveal the adsorption conditions of the silane coupling agents of metal oxide nanoparticles.

**Acknowledgments**

Financial support from the DIC, Chiba (Japan), is gratefully acknowledged. We thank the Japan Analytical Industry for providing us with the opportunity to use a Curie-point injector.

Analytical Methods Accepted Manuscript

## References

- 1 U. Diebold, *Surf. Sci. Rep.*, 2003, **48**, 53.
- 2 N. Sadrieh, A. M. Wokovich, N. V. Gopee, J. Zheng, D. Haines, D. Parmiter, P. H. Siitonen, C. R. Cozart, A. K. Patri, S. E. McNeil, P. C. Howard, W. H. Doub and L. F. Buhse, *Toxicol. Sci.*, 2010, **115**, 156.
- 3 A. Fujishima, X. Zhang and D. A. Tryk, *Surf. Sci. Rep*, 2008, **63**, 515.
- 4 K. Takahashi, K. Tadanaga, M. Tatsumisago and A. Matsuda, *J. Am. Ceram. Soc.*, 2006, **89**, 3107.
- 5 K. Shiba, S. Sato and M. Ogawa, *Bull. Chem. Soc. Jpn.*, 2012, **85**, 1040.
- 6 X. W. Li, R. G. Song, Y. Jiang, C. Wang and D. Jiang, *Appl. Surf. Sci.*, 2013, **276**, 761.
- 7 T. Jesionowski, S. Binkowski and A. Krysztafkiewicz, *Dyes Pigment.*, 2005, **65**, 267.
- 8 C. Magnenet, D. Massiot, I. Klur and J. P. Coutures, *J. Mater. Sci.*, 2000, **35**, 115.
- 9 N. M. Wichner, J. Beckers, G. Rothenberg and H. Koller, *J. Mater. Chem.*, 2010, **20**, 3840.
- 10 I. Ueta, A. Mizuguchi, K. Tani, S. Kawakubo and Y. Saito, *Anal. Sci.*, 2014, **30**, 407.
- 11 J. Raskó and J. Kiss, *Appl. Catal. A-Gen.*, 2005, **287**, 252.
- 12 Y. Chen, A. Lin and F. Gan, *Appl. Surf. Sci.*, 2006, **252**, 8635.
- 13 N. Nakayama and T. Hayashi, *Colloid Surf. A-Physicochem. Eng. Asp*, 2008, **317**, 543.

- 1  
2  
3  
4  
5  
6  
7  
8  
9  
10  
11  
12  
13  
14  
15  
16  
17  
18  
19  
20  
21  
22  
23  
24  
25  
26  
27  
28  
29  
30  
31  
32  
33  
34  
35  
36  
37  
38  
39  
40  
41  
42  
43  
44  
45  
46  
47  
48  
49  
50  
51  
52  
53  
54  
55  
56  
57  
58  
59  
60
- 14 T. C.-K. Yang, S.-F. Wang, S. H.-Y. Tsai and S.-Y. Lin, *Appl. Catal. B-Environ*, 2001, **30**, 293.
- 15 C. Breitkopf, S. Matysik and H. Papp, *Appl. Catal. A-Gen.*, 2006, **301**, 1.
- 16 K. Ohishi, T. Sakamoto, J. Saikawa, N. Ishigaki, K. Tojo, Y. Ido, S. Hayashi, S. Ishiuchi, K. Misawa and M. Fujii, *Anal. Sci.*, 2013, **29**, 291.
- 17 D. M. Lubman and R. M. Jordan, *Anal. Chem.*, 1985, **56**, 373.
- 18 C. W. Wilkerson, Jr. S. M. Colby and J. P. Reilly, *Anal. Chem.*, 1989, **61**, 2669.
- 19 C.-H. Lin, Y. Murata and T. Imasaka, *Anal. Chem.*, 1996, **68**, 1153.
- 20 Y.-C. Chang and T. Imasaka, *Anal. Chem.*, 2013, **85**, 349.
- 21 B. K. Gullett, L. Oudejans, D. Tabor, A. Touati and S. Ryan, *Environ. Sci. Technol.*, 2012, **46**, 923.
- 22 T. Uchimura, Y. Hironaka and M. Mori, *Anal. Sci.*, 2013, **29**, 85.
- 23 C. Mullen, M. J. Coggiola and H. Oser, *J. Am. Soc. Mass Spectrom.*, 2009, **20**, 419.
- 24 U. Boesl, A. Bornschlegl, C. Logé and K. Titze, *Anal. Bioanal. Chem.*, 2013, **405**, 6913.
- 25 T. Kuraishi and T. Uchimura, *Anal. Chem.*, 2013, **85**, 3493.
- 26 T. Uchimura and T. Imasaka, *Anal. Chem.*, 2000, **72**, 2648.



- 1  
2  
3  
4  
5  
6  
7  
8  
9  
10  
11  
12  
13  
14  
15  
16  
17  
18  
19  
20  
21  
22  
23  
24  
25  
26  
27  
28  
29  
30  
31  
32  
33  
34  
35  
36  
37  
38  
39  
40  
41  
42  
43  
44  
45  
46  
47  
48  
49  
50  
51  
52  
53  
54  
55  
56  
57  
58  
59  
60
- 27 R. Geissler, M. R. Saraji-Bozorgzad, T. Gröger, A. Fendt, T. Streibel, M. Sklorz, B. M. Krooss, K. Fuhrer, M. Gonin, E. Kaisersberger, T. Denner and R. Zimmermann, *Anal. Chem.*, 2009, **81**, 6038.
- 28 A. H. Falkovich and Y. Rudich, *Environ. Sci. Technol.*, 2001, **35**, 2326.
- 29 T. Yuzawa, A. Hosaka, C. Watanabe and S. Tsuge, *Anal. Sci.*, 2008, **24**, 953.
- 30 M. Kawaguchi, Y. Ishii, N. Sakui, N. Okanouchi, R. Ito, K. Saito and H. Nakazawa, *Anal. Chim. Acta*, 2005, **533**, 57.
- 31 T. Streibel, J. Weh, S. Mitschke and R. Zimmermann, *Anal. Chem.*, 2006, **78**, 5354.
- 32 T. Streibel, S. Mitschke, T. Adam, J. Weh and R. Zimmermann, *J. Anal. Appl. Pyrol.*, 2007, **79**, 24.
- 33 T. Nakaza, A. Kobayashi, T. Hirano, S. Kitagawa and H. Ohtani, *Anal. Sci.*, 2012, **28**, 917.
- 34 N. Oguri, T. Takeda, M. Endo and T. Tsuchiya, *Bunseki Kagaku*, 2013, **62**, 223.
- 35 S. Sakurai and T. Uchimura, *Anal. Sci.*, 2014, **30**, 891.
- 36 R. Tembreull, C. H. Sin, P. Li, H. M. Pang and D. M. Lubman, *Anal. Chem.*, 1985, **57**, 1186.
- 37 E. R. E. van der Hage, J. J. Boon, R. J. J. M. Steenvoorden and T. L. Weeding, *Anal. Chem.*, 1994, **66**, 543.

Figure Captions

Figure 1. Schematic representation of LI/TOFMS using a GC oven for pyrolysis of TiO<sub>2</sub> nanoparticles.

Figure 2. 266 nm nanosecond mass spectrum of PTES.

Figure 3. Two-dimensional display of the pyrolysis products of silanized TiO<sub>2</sub> nanoparticles heated by a GC oven obtained using LI/TOFMS. (a) 1.5 mg/g-TiO<sub>2</sub>, (b) 6.1 mg/g-TiO<sub>2</sub>. Time courses obtained by extracting at *m/z* 78, 118, and 132 are also shown. It should be mentioned that a few peaks were found at approximately 6 – 8.5 min. The peaks are marked with an asterisk (\*). They also were observed in a blank experiment, and probably arose from the glass fiber filter that was used as a cover.

Figure 4. Two-dimensional display of the pyrolysis products of 6.1 mg/g-TiO<sub>2</sub> nanoparticles obtained using a Py-GC/LI/TOFMS.

Figure 5. Mass chromatograms of PTES-dropped  $\text{TiO}_2$  nanoparticles (a) and a PTES-dropped glass fiber filter (b) obtained by extracting the data corresponding to benzene ( $m/z$  78) and PTES ( $m/z$  240).

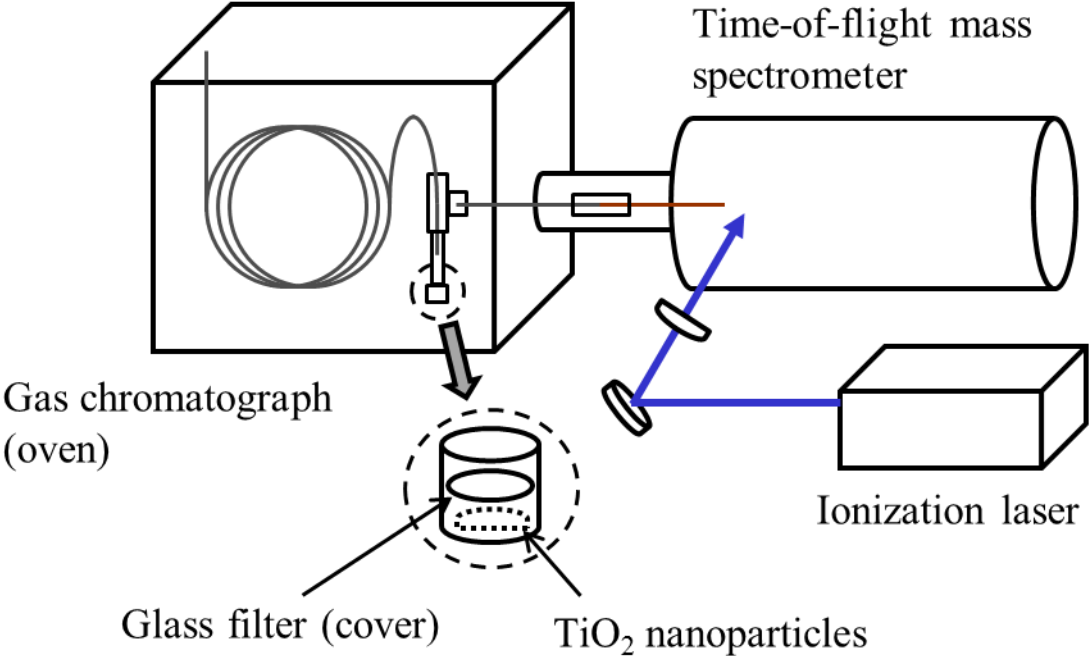


Fig. 1. T. Fujii et al.

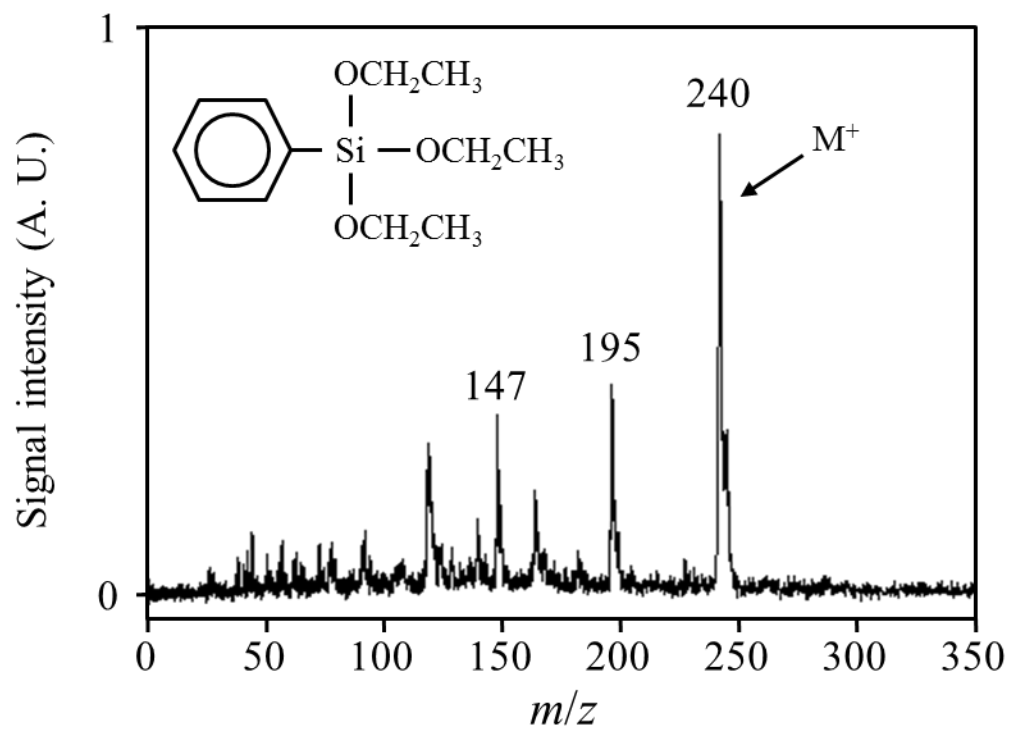


Fig. 2. T. Fujii et al.

1  
2  
3  
4  
5  
6  
7  
8  
9  
10  
11  
12  
13  
14  
15  
16  
17  
18  
19  
20  
21  
22  
23  
24  
25  
26  
27  
28  
29  
30  
31  
32  
33  
34  
35  
36  
37  
38  
39  
40  
41  
42  
43  
44  
45  
46  
47  
48  
49  
50  
51  
52  
53  
54  
55  
56  
57  
58  
59  
60

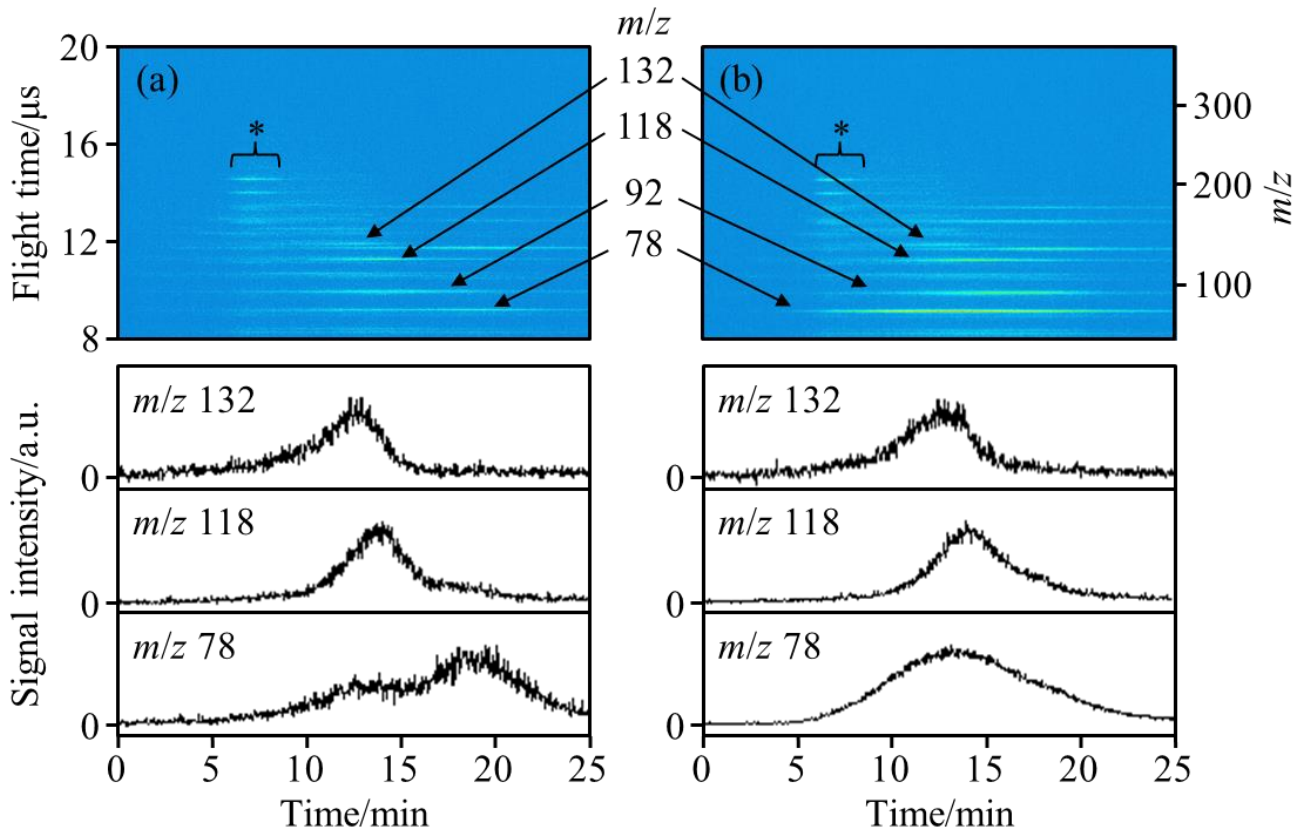


Fig. 3. T. Fujii et al.

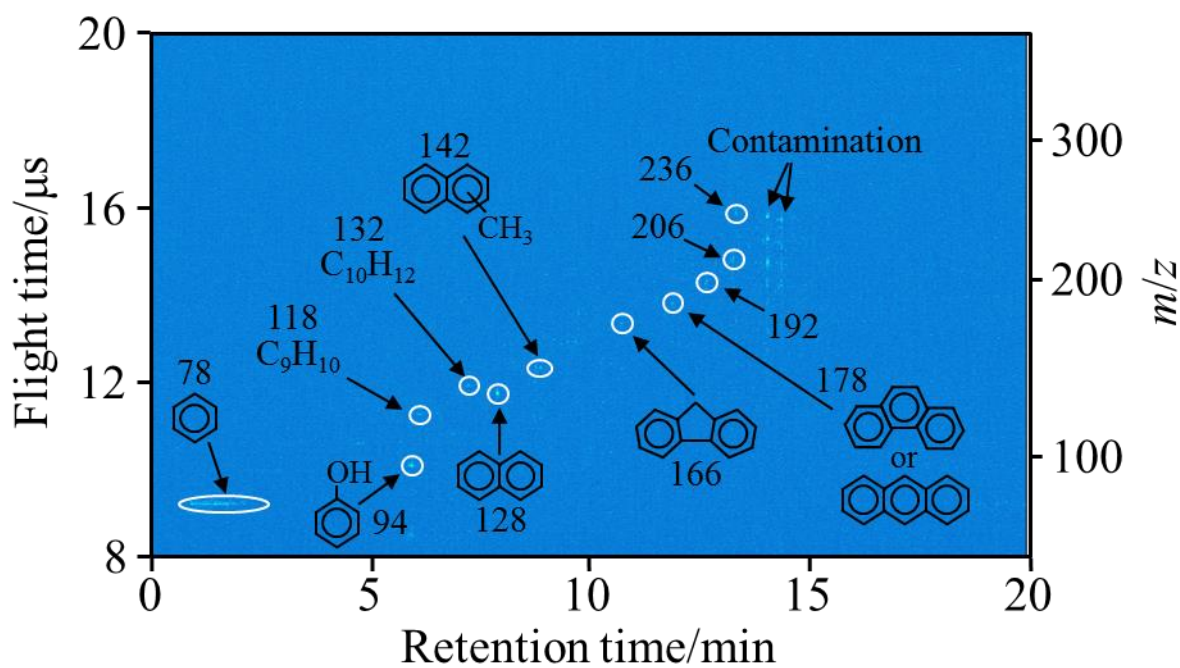


Fig. 4. T. Fujii et al.

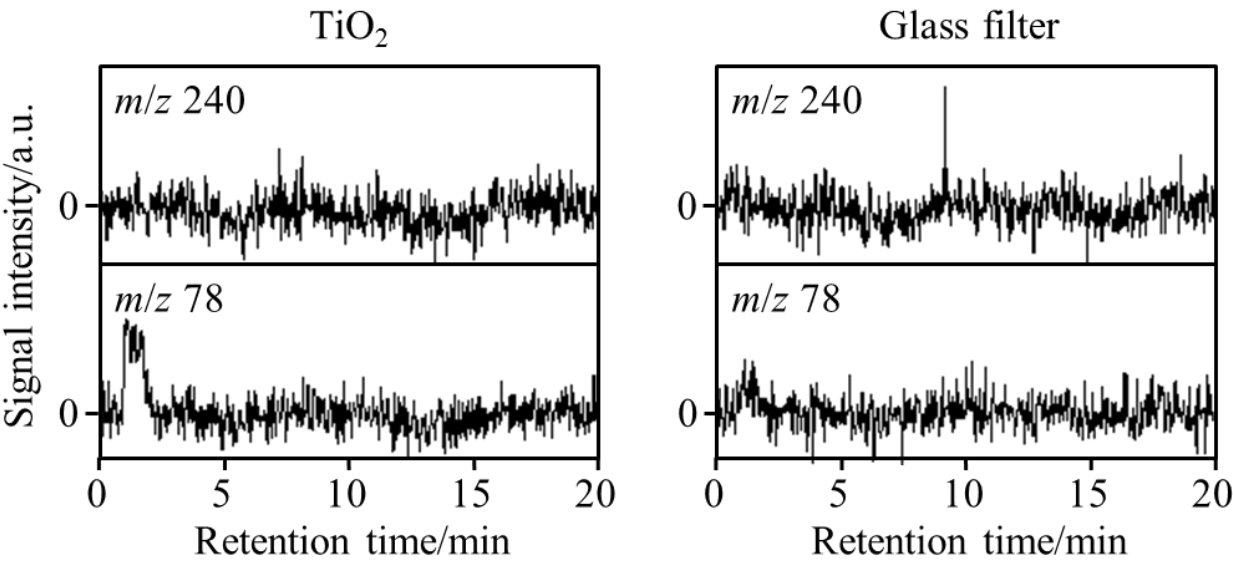


Fig. 5. T. Fujii et al.